12-1-2020

Fractional nonlinear Volterra–Fredholm integral equations involving Atangana–Baleanu fractional derivative: framelet applications

Mutaz Mohammad
Zayed University

Alexander Trounev
Kuban State Agrarian University

Mohammad and Trounev *Advances in Difference Equations* (2020) 2020:618
https://doi.org/10.1186/s13662-020-03042-9

Advances in Difference Equations
a SpringerOpen Journal

RESEARCH

Open Access

Fractional nonlinear Volterra–Fredholm integral equations involving Atangana–Baleanu fractional derivative: framelet applications

Mutaz Mohammad[1*] and Alexander Trounev[2]

*Correspondence:
Mutaz.Mohammad@zu.ac.ae
[1]Department of Mathematics, Zayed University, Abu Dhabi, UAE
Full list of author information is available at the end of the article

Abstract

In this work, we propose a framelet method based on B-spline functions for solving nonlinear Volterra–Fredholm integro-differential equations and by involving Atangana–Baleanu fractional derivative, which can provide a reliable numerical approximation. The framelet systems are generated using the set of B-splines with high vanishing moments. We provide some numerical and graphical evidences to show the efficiency of the proposed method. The obtained numerical results of the proposed method compared with those obtained from CAS wavelets show a great agreement with the exact solution. We confirm that the method achieves accurate, efficient, and robust measurement.

Keywords: Framelets; Numerical solution; Fractional calculus; Atangana–Baleanu fractional derivative; Wavelets; Harmonic numerical analysis; Volterra integral equations; Oblique extension principle

1 Introduction

Recently, many scientists have applied fractional derivatives with different types of definitions, such as Atangana–Baleanu fractional integral [1], Caputo fractional derivative [2], and Caputo–Fabrizio fractional derivative [3], to many real-world problems and pointed out the powerfulness of using such noninteger-order and nonlocal kernels to numerically solve different types of integral equations and to describe the dynamics and properties of these problems; see, for example, [4–37].

One of these problems is studying numerical solution of the nonlinear Volterra–Fredholm integral equations by involving the well-known Atangana–Baleanu fractional derivative. Note that nonlinear Volterra–Fredholm integral equations appear in many applications in different disciplines such as neural networks [38], the pulses of sound reflections [39], and mathematical physics such as Lane–Emden-type equations [40], and many more can be found, for example, in [41] and references therein. On the other hand, finding exact solutions of such equations is usually difficult and sometimes even impossible. Therefore developing numerical algorithms to simulate exact solutions with this new involvement of noninteger order is crucial.

There are many numerical methods for solving Fredholm and Voltera integral equations, such as the Galerkin method, collocation method, Taylor series, Legendre wavelets, Taylor and recently Chebyshev polynomials, homotopy perturbation method, power series method, and expansion method [42–48]. Besides these contributions, other authors have also applied wavelet bases and gained much attention during the last decade. However, these bases are typically nonredundant, and thus corruption or loss of transform coefficients can be serious. Motivated by the above, our main goal in this work is to propose a new efficient method based on framelet systems to numerically solve fractional nonlinear Volterra and Fredholm integral equations by involving the Atangana–Baleanu fractional order derivative. Framelet theory is a relatively emerging area in mathematical analysis and known as redundant systems. The redundancy of the framelet system requires that a given function would be represented by a different structure as a convergent sum. These expansions have recently emerged as another effective tool and popular through the use in numerous applications. One of the major advantages of a redundant system is that it is implemented by a frame fast transform, which provides us with better recovery and higher accuracy order. Indeed, one of our main contributions in this work is simulation of the solution of a given fractional nonlinear Volterra and Fredholm integral equation based on these framelet expansions (redundant setting). This means that the right representation is critical if we intend to effectively perform our solution.

A framelet system contains a set of functions called generators. We construct them using some known and effective principles such as the unitary and oblique extension principles (of course, including their generalizations) and based on nonnegative functions called B-splines. This provides us with simple and better reconstruction of the coefficients to obtain the corresponding unknown elements of the space $L^2(\mathbb{R})$ and also gives us better accuracy order and relatively small errors. In practice, framelet-based methods have been applied to provide accurate and efficient numerical schemes for solving several types of integral and differential equations; see, for example, [49–59].

We consider the following form of fractional nonlinear Volterra–Fredholm integral equation (FV-FIE):

$$\begin{aligned}\mathcal{D}^{\lambda}u(x) = g(x) + a\int_0^x \mathcal{K}_1(x,t)\mathcal{P}_1\big(u(t)\big)\,dt \\ + b\int_0^1 \mathcal{K}_1(x,t)\mathcal{P}_2\big(u(t)\big)\,dt, \quad x\in[0,1], \lambda>0,\end{aligned} \tag{1.1}$$

with initial conditions (ICs)

$$u^{(p)}(0) = d_p, \quad p = 0,1,2,\dots,m-1, \text{and } \lambda\in(n,n+1], n\in\mathbb{N}, \tag{1.2}$$

where $\mathcal{D}^{\lambda}u$ is the Atangana–Baleanu fractional-order derivative given by

$$\mathcal{D}^{\lambda}u(x) = \frac{M(\lambda)}{1-\lambda}\int_0^x \frac{du(t)}{dt}E_{\lambda}\left(\frac{-\lambda(x-t)^{\lambda}}{1-\lambda}\right)dt,$$

where $M(\lambda)$ is a normalization function satisfying $M(0) = M(1) = 1$, and E_λ is the Mittag-Leffler function. The integral operator corresponding to this definition is given by

$$\mathcal{I}^\lambda u(x) = \frac{(1-\lambda)u(x)}{M(\lambda)} + \frac{\lambda}{M(\lambda)\Gamma(\lambda)} \int_0^x \frac{u(t)}{(x-t)^{1-\lambda}}. \tag{1.3}$$

We refer the reader to [1, 13, 60, 61] for more details and properties of the fractional derivative.

The paper is organized as follows. In Sect. 2, we provide some preliminaries and basics of frames with necessary theory needed for the construction of the framelet systems. In Sect. 3, we establish a matrix formulation of the proposed method based on the constructed framelet systems and using the collocation technique. Numerical examples with numerical comparison and graphical illustration are presented in Sect. 4 to validate our main expansion technique.

2 Framelet expansion method

The purpose in this section is providing an approximate solution of the FV-FIE given in Equations (1.1)–(1.2) in the form of truncated expansions of a given framelet system.

A set of functions

$$\{u_j, j = 1, \dots, \infty\}$$

is called a frame for $L^2(\mathbb{R})$ if there exists positive numbers A, B such that

$$A\|v\|^2 \le \sum_{j=1}^{\infty} \bigl|\langle v, u_j\rangle\bigr|^2 \le B\|v\|^2 \tag{2.1}$$

for all functions $v \in L^2(\mathbb{R})$. The set is called tight frame (or framelet) if it is possible to have $A = B$.

Note that, according to inequality (2.1), for a function $g \in L^2(\mathbb{R})$, we obviously obtain the following associated framelet representation:

$$g = \sum_{j\in\mathbb{Z}} \langle g, u_j\rangle u_j. \tag{2.2}$$

The framelets are constructed using B-spline functions. The B-splines B_M of order M, where $M \in \mathbb{N}$, are recursively defined by the equation

$$B_M(x) = \int_0^1 B_{M-1}(x-t)\,dt, \quad M = 1, 2, \dots,$$

where $B_1(x)$ is the indicator function over the interval $[0, 1)$.

The Fourier transform of an integrable function f, denoted by $\hat{f}$, is defined by

$$\hat{f}(\omega) = \int_{\mathbb{R}} f(t)e^{-2\pi i\omega t}\,d\omega,$$

and the discrete Fourier series of a sequence $a(k)$, denoted by $\hat{a}$, is given by

$$\hat{a}(\omega) = \sum_{k=0}^{M-1} a(k) e^{2\pi i k\omega/M}.$$

B-splines are nonnegative refinable functions in the sense that

$$\widehat{B}_M(\omega) = \hat{a}(\omega/2)\hat{\phi}(\omega/2),$$

with

$$\hat{a}(\omega) = 2^{-n}\bigl(1 + \mathbf{e}^{-i\omega}\bigr)^n p(\omega), \tag{2.3}$$

where $p(\omega)$ is a polynomial of trigonometric functions with $p(0) = 1$, and $\hat{a}$ is a 2π-periodic function in the frequency domain, called the low mask of B_M.

The framelet system $X(\Omega)$ is constructed via the oblique extension principle (OEP) [49] and it has the form

$$X(\Omega) = \bigl\{u_{\ell,j,k} = 2^{j/2} u\bigl(2^j x - k\bigr) : \ell = 1, \ldots, r; j, k \in \mathbb{Z}\bigr\} \tag{2.4}$$

and satisfies the following equations:

$$\sum_{\ell=0}^{r} \bigl|\hat{a}_\ell(\omega)\bigr|^2 = 1 \quad \text{and} \quad \sum_{\ell=0}^{r} \hat{a}_\ell(\omega)\hat{a}_\ell(\omega + \pi) = 0, \tag{2.5}$$

where $\hat{a}_0$, $\hat{a}_\ell$, $\ell = 1, \ldots, r$, are the low and high masks of $u = B_M$, respectively. The OEP deals with the notion of constructing a framelet system using a refinable function ϕ where for some trigonometric function $\hat{\Omega}(\omega)$,

- $\hat{\Omega}(\omega)|\hat{\phi}(0)|^2 = 1$, and
- $\hat{\Omega}(\omega)\hat{a}(\omega/2 + \pi i)\overline{\hat{a}(\omega/2)} + \sum_{\ell\in E} \hat{a}_\ell(\omega/2 + \pi i)\overline{\hat{a}_\ell(\xi/2)} = \Omega(\cdot/2)\delta_i$, $\{i : i = 0, 1\}$.

Then the system $X(\Omega)$ defined in Equation (2.4) forms a framelet system for $L_2(\mathbb{R})$. The representation in Equation (2.2) is truncated by the series $\mathcal{W}_n$ such that

$$\mathcal{W}_n g = \sum_{\ell=1}^{r} \sum_{j=-n}^{n} \sum_{k\in\mathbb{Z}} c_{\ell,j,k} u_{\ell,j,k}, \tag{2.6}$$

where $c_{\ell,j,k} = \langle g, u_{\ell,j,k}\rangle$.

Let us present some examples of framelet systems via the OEP setting.

Example 2.1 Consider the refinable function $B_2(x)$. Then, based on the OEP presented in [49], we are able to explicitly construct the following framelets:

$$\hat{\psi}_1(\omega) = -\frac{16e^{-\frac{1}{2}(i\omega)}}{\omega^2} - \frac{16e^{-\frac{1}{2}(3i\omega)}}{\omega^2} + \frac{24e^{-i\omega}}{\omega^2} + \frac{4e^{-2i\omega}}{\omega^2} + \frac{4}{\omega^2} + \frac{1}{\sqrt{2\pi}},$$

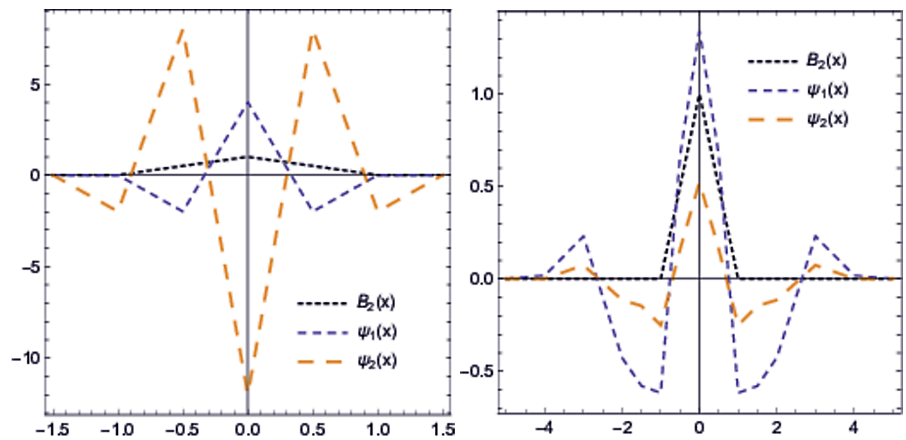

Figure 1 The graphs of the functions in $X(\Omega_1)$ for Examples 2.1 and 2.2, respectively

$$\hat{\psi}_2(\omega) = \frac{2\sqrt{\frac{2}{\pi}}e^{\frac{i\omega}{2}}}{\omega^2} + \frac{30\sqrt{\frac{2}{\pi}}e^{-\frac{1}{2}(i\omega)}}{\omega^2} + \frac{30\sqrt{\frac{2}{\pi}}e^{-\frac{1}{2}(3i\omega)}}{\omega^2} + \frac{2\sqrt{\frac{2}{\pi}}e^{-\frac{1}{2}(5i\omega)}}{\omega^2} - \frac{40\sqrt{\frac{2}{\pi}}e^{-i\omega}}{\omega^2} - \frac{12\sqrt{\frac{2}{\pi}}e^{-2i\omega}}{\omega^2} - \frac{12\sqrt{\frac{2}{\pi}}}{\omega^2}.$$

Then according to the OEP, the set $X(\Omega_1)$ where $\Omega_1 = \{\psi_1, \psi_2\}$ forms a framelet system for $L^2(\mathbb{R})$. The graph of the generators of the corresponding framelet system is given in Fig. 1 (the left subfigure).

Example 2.2 Consider the refinable function $B_4(x)$. Then, again based on the OEP, we have

$$\begin{aligned}
\hat{\psi}_1(\omega) = {}& \frac{e^{-i\omega}}{1920\omega^2}\left(4720\cos\left(\frac{\omega}{2}\right) - 880\cos\left(\frac{3\omega}{2}\right)\right. \\
& - 10{,}178\cos(\omega) - 1352\cos(2\omega) + 3337\cos(3\omega) \\
& \left. - 742\cos(4\omega) - 71\cos(5\omega) + 5166\right), \\
\hat{\psi}_2(\omega) = {}& \frac{1}{960\sqrt{2\pi}\omega^2}\left(-1 + e^{-\frac{1}{2}(i\omega)}\right)^4 \\
& \times \left(-726e^{-\frac{1}{2}(i\omega)}\left(1 + e^{i\omega}\right) + 85\left(e^{-i\omega} + e^{i\omega}\right) + 458\left(e^{-2i\omega} + e^{2i\omega}\right)\right. \\
& \left. + 412e^{-\frac{1}{2}(3i\omega)}\left(1 + e^{3i\omega}\right) + 71\left(e^{-3i\omega} + e^{3i\omega}\right) + 284e^{-\frac{1}{2}(5i\omega)}\left(1 + e^{5i\omega}\right) - 1228\right).
\end{aligned}$$

Therefore the set $X(\Omega_2)$ where $\Omega_2 = \{\psi_1, \psi_2\}$ forms a framelet system for $\in L^2(\mathbb{R})$. The graph of the generators of the corresponding framelet system is plotted in Fig. 1 (the right subfigure).

3 Matrix formulation using framelets

In this section, we provide a general framework of the proposed algorithm based on the collocation division of the domain.

Consider the FV-FIE defined in Equation (1.1). Based on the truncated expansion obtained in Equation (2.6), we have

$$\frac{M(\lambda)}{1-\lambda}\int_0^x \frac{d\mathcal{W}(u_m(t))}{dt}E_\lambda\left(\frac{-\lambda(x-t)^\lambda}{1-\lambda}\right)dt = g(x) + a\int_0^x \mathcal{K}_1(x,t)\mathcal{I}^\lambda\mathcal{P}_1\big(\mathcal{W}_m u(t)\big)\,dt \\ + b\int_0^1 \mathcal{K}_1(x,t)\mathcal{I}^\lambda\mathcal{P}_2\big(\mathcal{W}_m u(t)\big)\,dt, \qquad (3.1)$$

where $\mathcal{I}^\lambda$ is the Riemann–Liouville fractional-integral operator defined by Equation (1.3).

With a few algebra, Equation (3.1) can be simplified to

$$\begin{aligned}
&\frac{M(\lambda)}{1-\lambda}\int_0^x \frac{d\mathcal{W}(u_m(t))}{dt}E_\lambda\left(\frac{-\lambda(x-t)^\lambda}{1-\lambda}\right)dt \\
&\quad= g(x) + a\int_0^x \mathcal{K}_1(x,t)\frac{(1-\lambda)\mathcal{P}_1(\mathcal{W}_m u(x))}{M(\lambda)}\,dt \\
&\qquad+ \frac{\lambda}{M(\lambda)\Gamma(\lambda)}\int_0^x\int_0^t \frac{\mathcal{P}_1(\mathcal{W}_m u(s))}{(x-s)^{1-\lambda}}\,ds\,dt + b\int_0^1 \mathcal{K}_2(x,t)\frac{(1-\lambda)\mathcal{P}_2(\mathcal{W}_m u(x))}{M(\lambda)}\,dt \\
&\qquad+ \frac{\lambda}{M(\lambda)\Gamma(\lambda)}\int_0^1\int_0^x \frac{\mathcal{P}_2(\mathcal{W}_m u(t))}{(x-t)^{1-\lambda}}\,ds.
\end{aligned}$$

Hence,

$$\begin{aligned}
&\frac{M(\lambda)}{1-\lambda}\int_0^x \frac{d\mathcal{W}(u_m(t))}{dt}E_\lambda\left(\frac{-\lambda(x-t)^\lambda}{1-\lambda}\right)dt - a\int_0^x \mathcal{K}_1(x,t)\frac{(1-\lambda)\mathcal{P}_1(\mathcal{W}_m u(x))}{M(\lambda)}\,dt \\
&\quad+ \frac{\lambda}{M(\lambda)\Gamma(\lambda)}\int_0^x\int_0^t \frac{\mathcal{P}_1(\mathcal{W}_m u(s))}{(x-s)^{1-\lambda}}\,ds\,dt - b\int_0^1 \mathcal{K}_2(x,t)\frac{(1-\lambda)\mathcal{P}_2(\mathcal{W}_m u(x))}{M(\lambda)}\,dt \\
&\quad- \frac{\lambda}{M(\lambda)\Gamma(\lambda)}\int_0^1\int_0^x \frac{\mathcal{P}_2(\mathcal{W}_m u(t))}{(x-t)^{1-\lambda}}\,ds = g(x).
\end{aligned}$$

Now, based on a dyadic division points of the domain of the framelet system used, say $\{\xi_q, q\in\Delta\}$, plugging these points into this equation, we have

$$\begin{aligned}
&\frac{M(\lambda)}{1-\lambda}\int_0^{\xi_q} \frac{d\mathcal{W}(u_m(t))}{dt}E_\lambda\left(\frac{-\lambda(\xi_q-t)^\lambda}{1-\lambda}\right)dt - a\int_0^{\xi_q} \mathcal{K}_1(x,t)\frac{(1-\lambda)\mathcal{P}_1(\mathcal{W}_m u(x))}{M(\lambda)}\,dt \\
&\quad- \frac{\lambda}{M(\lambda)\Gamma(\lambda)}\int_0^{\xi_q}\int_0^t \frac{\mathcal{P}_1(\mathcal{W}_m u(s))}{(\xi_q-s)^{1-\lambda}}\,ds\,dt \\
&\quad- b\int_0^1 \mathcal{K}_2(\xi_q,t)\frac{(1-\lambda)\mathcal{P}_2(\mathcal{W}_m u(\xi_q))}{M(\lambda)}\,dt \\
&\quad- \frac{\lambda}{M(\lambda)\Gamma(\lambda)}\int_0^1\int_0^{\xi_q} \frac{\mathcal{P}_2(\mathcal{W}_m u(t))}{(\xi_q-t)^{1-\lambda}}\,ds = g(\xi_q).
\end{aligned}$$

By approximating the integrals in this equation based on the composite trapezoidal rule, we get a generated system of equations, which can be solved to obtain the unknown coefficients $c_{\ell,j,k}$, as in Equation (2.6), in order to have an approximated solution of order m.

4 Numerical applications

In this section, we consider some examples to test the proposed algorithm. The absolute errors are given by

$$\mathcal{E}_m u = \left|u - \mathcal{I}^n(\mathcal{P}_m u)\right|, \quad \lambda \le n.$$

For comparison, we provide some numerical results for Example 4.1 based on Cos and Sin (CAS) wavelets defined by

$$\tau_{a,b}(x) = 2^{a/2}\,\mathrm{SAC}_p\big(2^a x - (b-1)\big), \quad 2^{-a}(b-1) \le x \le 2^{-a} b,$$

and based on the collocation method, where the translation parameter is given by

$$\mathrm{SAC}_p(x) = \cos(2p\pi x) + \sin(2p\pi x), \quad b = 1, \dots, 2^a.$$

The truncated expansion using such bases is given by

$$\mathcal{M}u(x) = \sum_{n=0}^{2^k-1} \sum_{p=-p^*}^{p^*} d_{np^*}\tau_{np^*}(x).$$

Example 4.1 Consider the FVIE

$$\begin{cases} \frac{M(\lambda)}{1-\lambda}\int_0^x \frac{d\mathcal{P}u_m(t)}{dt} E_\lambda\big(\frac{-\lambda(x-t)^\lambda}{1-\lambda}\big)\,dt - \int_0^x e^{-t}(\mathcal{I}^n(\mathcal{P}_m u)^2(t)\,dt = 1, \\ u(0) = 1, \\ u'(0) = 1, \\ u''(0) = 1, \\ u'''(0) = 1, \end{cases} \tag{4.1}$$

where

$$M(\lambda) = \frac{\Gamma(\lambda)(1-\lambda) + \lambda}{\Gamma(\lambda)}.$$

The exact solution solution is $u(x) = e^x$, where $\lambda = 4$. Applying the above algorithm yields the numerical results presented in Tables 1, 2, and 3. Graphical illustrations using different values of λ to compare the results between the exact and approximate solutions are also given in Figs. 2, 3, 4, and 5.

Example 4.2 Let us consider the following nonlinear equation, which appears in some applications of Newtonian gravity:

$$u''(x) + 2x^{-1}u'(x) + u^5(x) = 0$$

with ICs $u(0) = 1$ and $u'(0) = 0$. The equation can be transferred to the Volterra integral equation form

$$\begin{cases} u(x) - \frac{1}{x}\int_0^x (t^2 - tx)u^5(t)\,dt = 1, \\ u(0) = 1, \\ u'(0) = 0. \end{cases} \tag{4.2}$$

Table 1 Numerical results of Example 4.1 using the framelet systems $X(\Omega_1)$ and $X(\Omega_2)$ for $m = 3$ and $\lambda = 3.25$

x	Exact	$\mathcal{W}_m u$ via $X(\Omega_1)$	$\mathcal{W}_m u$ via $X(\Omega_2)$	$\mathcal{M}u, a = 3 = p^* = 3$
0.0	1.00000	1.00000	1.00000	1.00004
0.1	1.10527	1.10518	1.10527	1.10520
0.2	1.22140	1.22197	1.22206	1.22213
0.3	1.34986	1.35209	1.35215	1.35231
0.4	1.49182	1.49742	1.49750	1.49776
0.5	1.64872	1.66006	1.66024	1.66340
0.6	1.82212	1.84239	1.84268	1.84379
0.7	2.01375	2.04696	2.04731	2.04738
0.8	2.22554	2.27643	2.27683	2.27759
0.9	2.45960	2.53365	2.53415	2.53649
1.0	2.71828	2.84435	2.84432	2.84543

Table 2 Numerical results of Example 4.1 using the framelet systems $X(\Omega_1)$ and $X(\Omega_2)$ for $m = 3$ and $\lambda = 3.5$

x	Exact	$\mathcal{W}_m u$ via $X(\Omega_1)$	$\mathcal{W}_m u$ via $X(\Omega_2)$	$\mathcal{M}u, a = 3 = p^* = 3$
0.0	1.00000	1.00000	1.00000	1.00000
0.1	1.10527	1.10523	1.10534	1.10520
0.2	1.22140	1.22170	1.22180	1.22189
0.3	1.34986	1.35091	1.35223	1.35298
0.4	1.49182	1.49453	1.49722	1.49707
0.5	1.64872	1.65442	1.65998	1.65999
0.6	1.82212	1.83259	1.84239	1.84337
0.7	2.01375	2.03129	2.04661	2.04934
0.8	2.22554	2.25293	2.27630	2.27766
0.9	2.45960	2.50018	2.53316	2.54492
1.0	2.71828	2.73552	2.74283	2.75209

Table 3 Numerical results of Example 4.1 using the framelet systems $X(\Omega_1)$ and $X(\Omega_2)$ for $m = 3$ and $\lambda = 3.75$

x	Exact	$\mathcal{W}_m u$ via $X(\Omega_1)$	$\mathcal{W}_m u$ via $X(\Omega_2)$	$\mathcal{M}u, a = 3 = p^* = 3$
0.0	1.00000	1.00000	1.00000	1.00000
0.1	1.10527	1.10521	1.10514	1.10518
0.2	1.22140	1.22152	1.22146	1.22159
0.3	1.34986	1.35025	1.35022	1.35027
0.4	1.49182	1.49282	1.49280	1.49354
0.5	1.64872	1.65086	1.65077	1.65217
0.6	1.82212	1.82613	1.82599	1.82669
0.7	2.01375	2.02059	2.02044	2.02240
0.8	2.22554	2.23642	2.23628	2.23719
0.9	2.45960	2.47597	2.47582	2.47665
1.0	2.71828	2.72536	2.71663	2.73001

The exact solution is

$$u(x) = \frac{\sqrt{3}}{\sqrt{x^2 + 3}}.$$

In Figs. 6 and 7, we present some graphical illustrations to compare the exact and approximate solutions and error bounds.

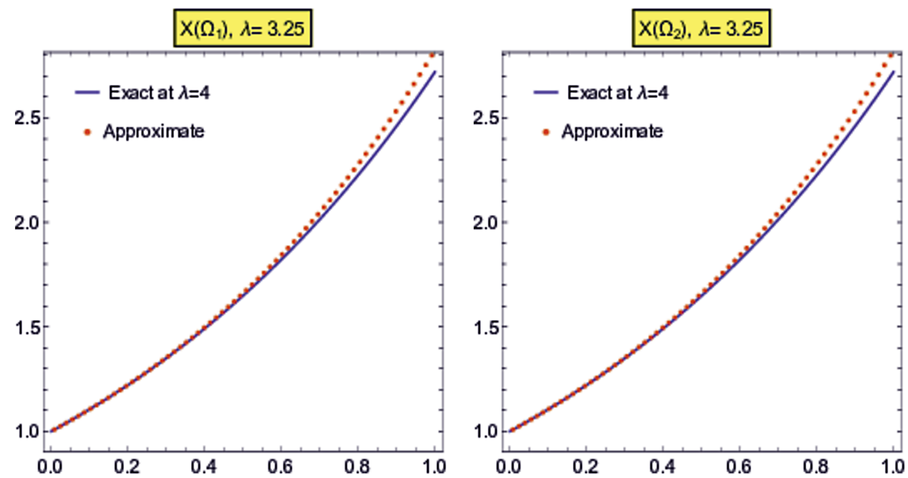

Figure 2 Comparison of the exact and approximate solutions of Example 4.1 for $m = 3$ and $\lambda = 3.25$

Figure 3 Comparison of the exact and approximate solutions of Example 4.1 for $m = 3$ and $\lambda = 3.25$ using the framelet systems $X(\Omega_1)$ and $X(\Omega_2)$

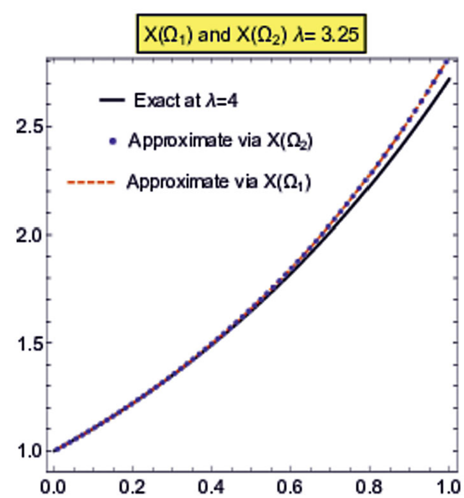

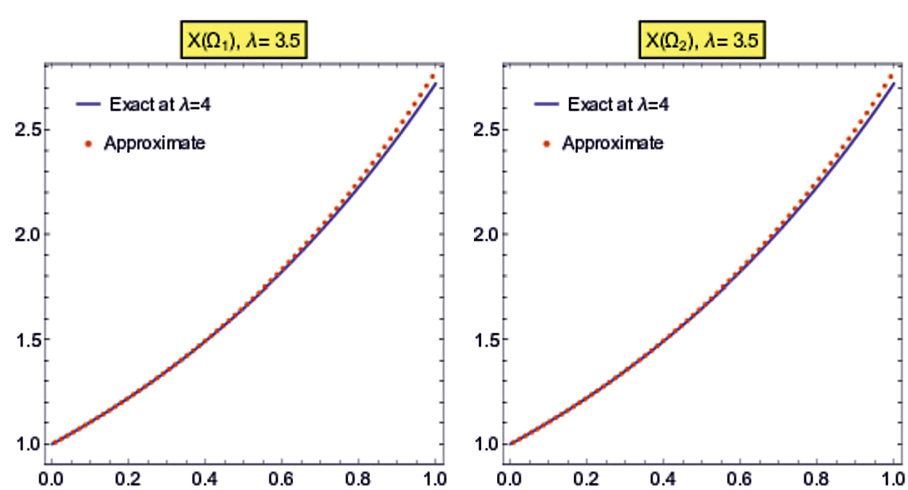

Figure 4 Comparison of the exact and approximate solutions of Example 4.1 for $m = 3$ and $\lambda = 3.5$

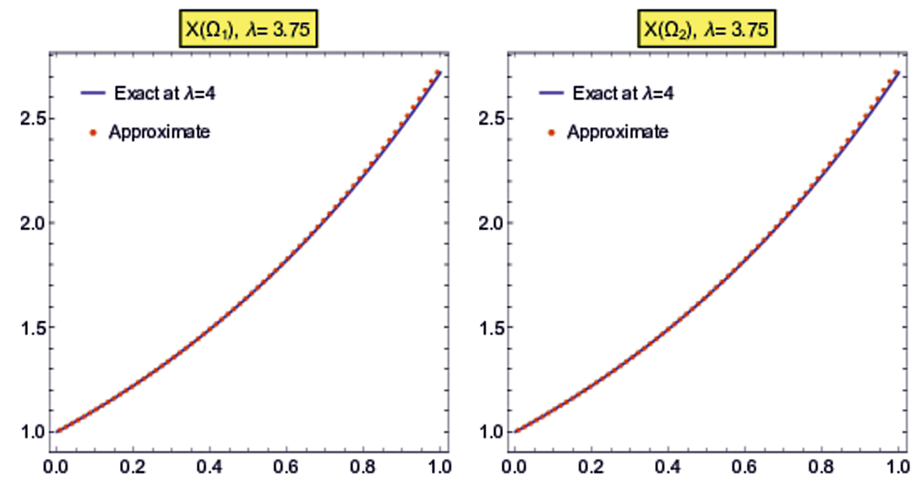

Figure 5 Comparison of the exact and approximate solutions of Example 4.1 for $m = 3$ and $\lambda = 3.75$

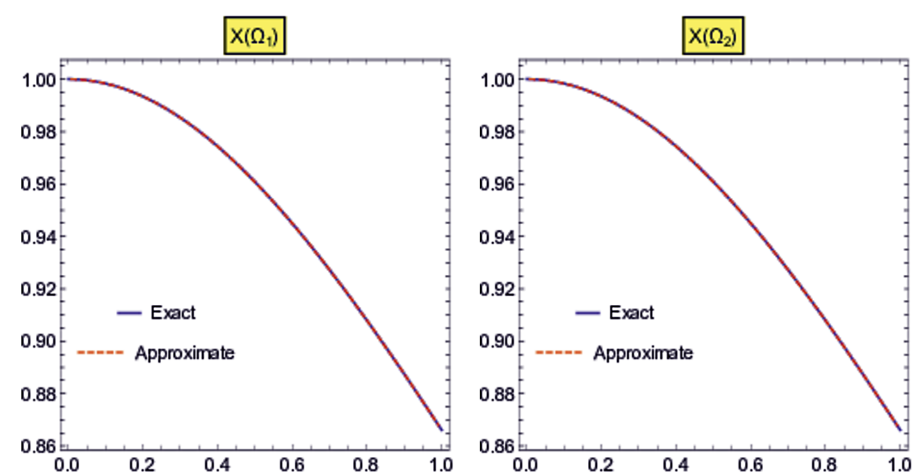

Figure 6 Comparison of the exact and approximate solutions of Example 4.2 for $m = 3$

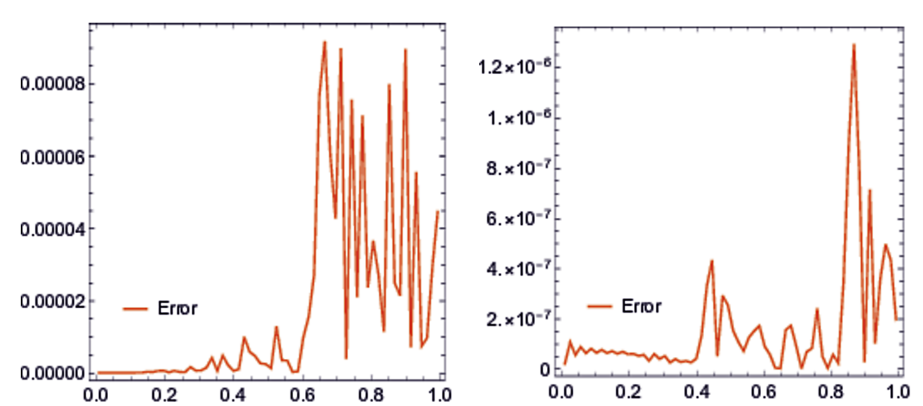

Figure 7 Comparison of the exact and approximate solutions of Example 4.2 for $m = 3$

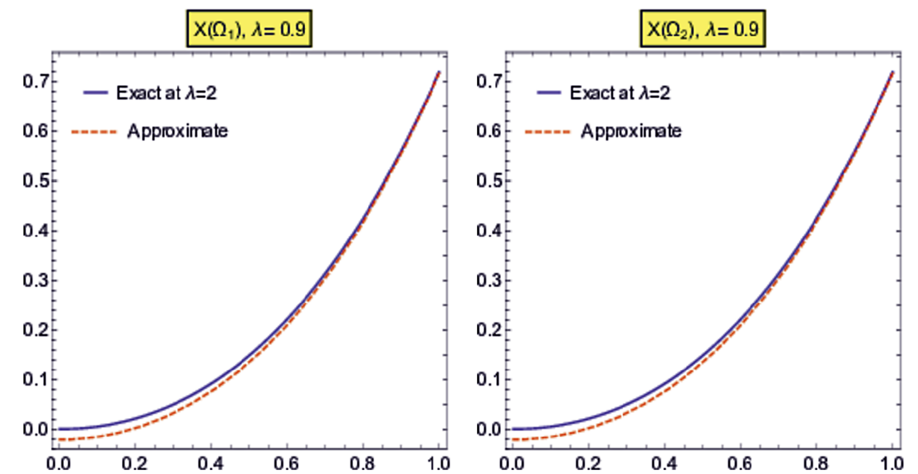

Figure 8 Comparison of the exact and approximate solutions of Example 4.3 for $m = 3$ and $\lambda = 0.9$

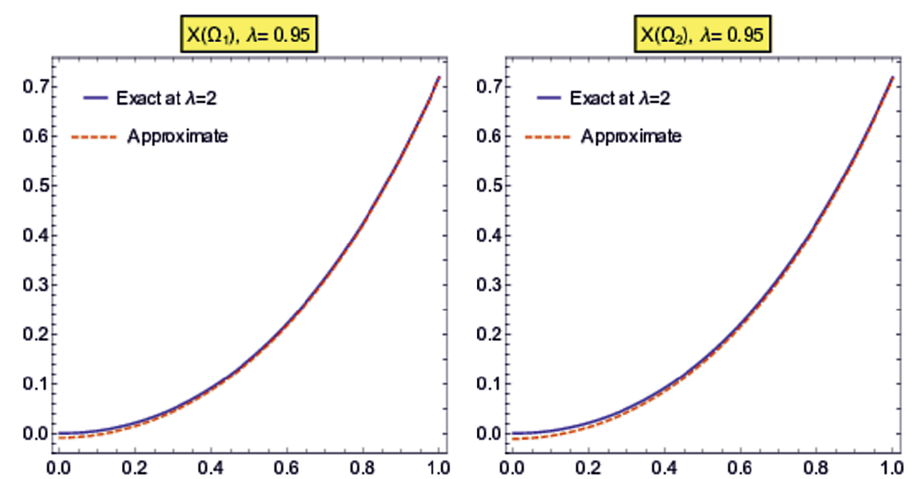

Figure 9 Comparison of the exact and approximate solutions of Example 4.3 for $m = 3$ and $\lambda = 0.95$

Example 4.3 We consider the following nonlinear fractional differential equation with mixed boundary conditions:

$$\begin{cases} D^{\lambda+1}u(x) - \int_0^1 xtu^6(t)\,dt - \int_0^x (e^t - 1)u^2(t)\,dt \\ \quad = -\frac{1}{3}(e^x - x - 1)^3 - (-2e + \frac{e^2}{4} + \frac{11}{3})x + e^x, \\ u(0) = -u'(0), \\ u(1) = u'(1) + 2e - 3, \end{cases} \tag{4.3}$$

where

$$D^{\lambda+1}u(x) = \frac{M(\lambda+1)}{2-\lambda}\int_0^x \frac{d\mathcal{P}u_m(t)}{dt} E_{\lambda+1}\left(\frac{-\lambda - 1(x-t)^{\lambda+1}}{2-\lambda}\right) dt.$$

The exact solution is $u(x) = e^x - x - 1$. The graphical illustrations are given in Figs. 8 and 9.

Table 4 Numerical results of Example 4.4 using the framelet systems $X(\Omega_1)$ and $X(\Omega_2)$ for $m = 3$ and $\lambda = 6/5$

x	Exact	$\mathcal{W}_m u$ via $X(\Omega_1)$	$\mathcal{W}_m u$ via $X(\Omega_2)$
0.0	0.00	0.0000611	0.000058
0.1	0.01	0.0073854	0.010312
0.2	0.04	0.0381471	0.038145
0.3	0.09	0.0835573	0.083556
0.4	0.16	0.1587530	0.158752
0.5	0.25	0.2578740	0.242248
0.6	0.36	0.3618780	0.361877
0.7	0.49	0.4834600	0.483460
0.8	0.64	0.6475220	0.647520
0.9	0.81	0.8071900	0.807188
1.0	1.00	0.9844360	0.984434

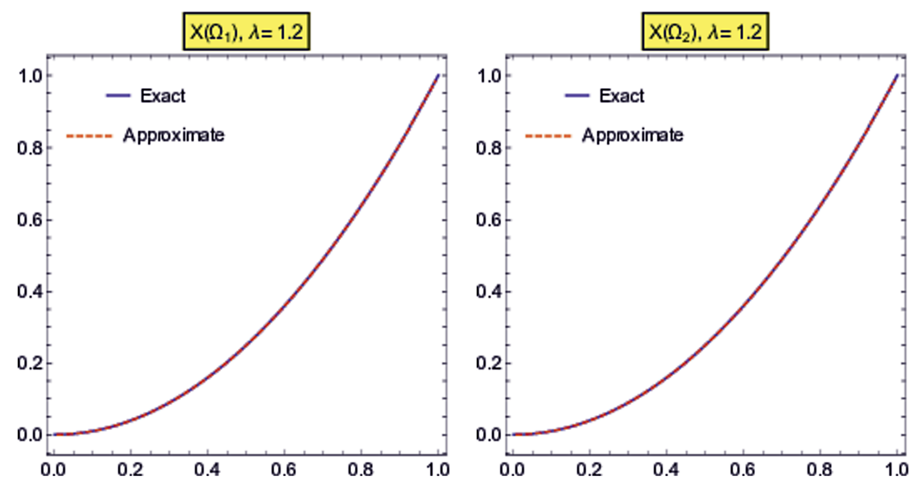

Figure 10 Comparison of the exact and approximate solutions of Example 4.4 for $m = 3$ and $\lambda = 1.2$

Example 4.4 Now, we consider the FVIE

$$\begin{cases} \frac{M(\lambda)}{1-\lambda}\int_0^x \frac{d\mathcal{P}u_m(t)}{dt}E_\lambda\left(\frac{-\lambda(x-t)^\lambda}{1-\lambda}\right)dt - \int_0^x (x-t)^2u^3(t)\,dt = -(x^9/252) + \frac{5x^{4/5}}{2\Gamma[4/5]}, \\ u(0) = 0, \\ u(1) = 1. \end{cases}$$

The exact solution for this equation when $\lambda = 6/5$ is $u(x) = x^2$. The numerical results of this example are presented in Table 4, and the graphical illustrations of the exact, approximate, and error results are depicted in Figs. 10 and 11.

5 Conclusion

In this work, we presented an efficient method based on framelet systems to solve nonlinear Volterra–Fredholm integral and integro-differential equations by involving the Atangana–Baleanu fractional derivative. We used some constructed framelet systems generated using the B-spline functions with high vanishing moments to numerically solve the related equations. We converted the considered problem given in Equation (1.1) to a matrix system after employing the Atangana–Baleanu fractional derivative definition,

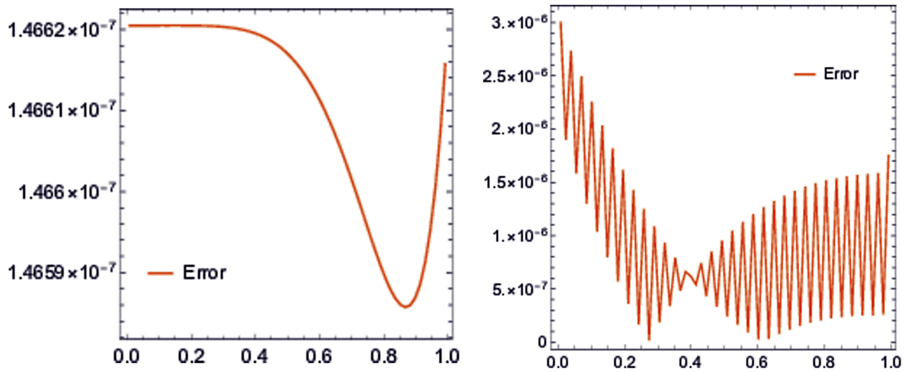

Figure 11 Error graphs of Example 4.4 for $m = 3$ and $\lambda = 1.2$ using framelet systems $X(\Omega_1)$ and $X(\Omega_2)$, respectively

where the resulted integrals are approximated using the composite trapezoidal rule. The obtained results indicate that the method produces high accuracy order and reliable results with only a few terms of the truncated framelet partial sums with a proper discretization. We have also supported our results by some graphical illustrations of the exact and approximate solutions and provided error bounds of the solved examples.

Acknowledgements
We would like to thank the reviewers for their thoughtful comments and efforts toward improving our manuscript.

Funding
This work was supported by the Research Office, Zayed University, STG Grant number STG064.

Availability of data and materials
Data sharing not applicable to this papere as no datasets were generated or analyzed during the current study.

Competing interests
The authors declare that they have no competing interests.

Authors' contributions
MM: Conceptualization, Methodology, Visualization, Investigation, Supervision, Validation, Software, Writing (review and editing). AT: Software and Validation. All authors read and approved the final manuscript.

Author details
[1]Department of Mathematics, Zayed University, Abu Dhabi, UAE. [2]Department of Computer Technology and Systems, Kuban State Agrarian University, Krasnodar, Russia.

Publisher's Note

Received: 10 July 2020 Accepted: 8 October 2020 Published online: 02 November 2020

References
1. Abdon, A., Dumitru, B.: New fractional derivatives with non-local and nonsingular kernel, theory and application to heat transfer model. Therm. Sci. **20**(1), 763–769 (2016). https://doi.org/10.2298/TSCI160111018A
2. Caputo, M.: Linear model of dissipation whose Q is almost frequency independent. Geophys. J. Int. **13**(5), 529–539 (1967). https://doi.org/10.1111/j.1365-246X.1967.tb02303.x
3. Caputo, M., Fabrizio, M.: A new definition of fractional derivative without singular kernel. Prog. Fract. Differ. Appl. **2**(1), 1–13 (2015). https://doi.org/10.12785/pfda/010201
4. Mohammad, M., Trounev, A.: On the dynamical modeling of Covid-19 involving Atangana–Baleanu fractional derivative and based on Daubechies framelet simulations. Chaos Solitons Fractals **140**, 110171 (2020). https://doi.org/10.1016/j.chaos.2020.110171
5. Mohammad, M., Trounev, A., Cattani, C.: An efficient method based on framelets for solving fractional Volterra integral equations. Entropy **22**(8), 824 (2020). https://doi.org/10.3390/e22080824
6. Mohammad, M., Cattani, C.: Applications of bi-framelet systems for solving fractional order differential equations. Fractals **28**, 2040051 (2020). https://doi.org/10.1142/S0218348X20400514

7. Mohammad, M., Cattani, C.: A collocation method via the quasi-affine biorthogonal systems for solving weakly singular type of Volterra–Fredholm integral equations. Alex. Eng. J. **59**(4), 2181–2191 (2020). https://doi.org/10.1016/j.aej.2020.01.046
8. Mohammad, M., Trounev, A., Cattani, C.: The dynamics of COVID-19 in the UAE based on fractional derivative modeling using Riesz wavelets simulation. Preprint (Version 1) (2020). https://doi.org/10.21203/rs.3.rs-33366/v1
9. Ghanbari, B., Atangana, A.: A new application of fractional Atangana–Baleanu derivatives: designing ABC-fractional masks in image processing. Phys. A, Stat. Mech. Appl. **542**, 123516 (2020). https://doi.org/10.1016/j.physa.2019.123516
10. Khan, M.A., Atangana, A.: Modeling the dynamics of novel coronavirus (2019-nCov) with fractional derivative. Alex. Eng. J. **59**(4), 2379–2389 (2020). https://doi.org/10.1016/j.aej.2020.02.033
11. Atangana, A., Bonyah, E., Elsadany, A.: A fractional order optimal 4D chaotic financial model with Mittag-Leffler law. Chin. J. Phys. **65**, 38–53 (2020). https://doi.org/10.1016/j.cjph.2020.02.003
12. Atangana, A., Aguilar, J., Kolade, M., Hristov, J.: Fractional differential and integral operators with non-singular and non-local kernel with application to nonlinear dynamical systems. Chaos Solitons Fractals **2020**, 109493 (2020). https://doi.org/10.1016/j.chaos.2019.109493
13. Atangana, A., Koca, I.: Chaos in a simple nonlinear system with Atangana–Baleanu derivatives with fractional order. Chaos Solitons Fractals **89**, 447–454 (2016)
14. Atangana, A.: On the new fractional derivative and application to nonlinear Fisher's reaction–diffusion equation. Appl. Math. Comput. **273**, 948–956 (2016)
15. Atangana, A., Aguilar, J.: Decolonisation of fractional calculus rules: breaking commutativity and associativity to capture more natural phenomena. Eur. Phys. J. Plus **133**, 166 (2018)
16. Ghanbari, B., Atangana, A.: Some new edge detecting techniques based on fractional derivatives with non-local and non-singular kernels. Adv. Differ. Equ. (2020). https://doi.org/10.1186/s13662-020-02890-9
17. Baleanu, D., Jajarmi, A., Mohammad, H., Rezapour, S.: A new study on the mathematical modelling of human liver with Caputo–Fabrizio fractional derivative. Chaos Solitons Fractals **134**, 109705 (2020)
18. Baleanu, D., Rezapour, S., Saberpour, Z.: On fractional integro-differential inclusions via the extended fractional Caputo–Fabrizio derivation. Bound. Value Probl. **2019**, 79 (2019)
19. Baleanu, D., Etemad, S., Rezapour, S.: A hybrid Caputo fractional modeling for thermostat with hybrid boundary value conditions. Bound. Value Probl. **2020**, 64 (2020). https://doi.org/10.1186/s13661-020-01361-0
20. Aydogan, M.S., Baleanu, D., Mousalou, A., et al.: On high order fractional integro-differential equations including the Caputo–Fabrizio derivative. Bound. Value Probl. **2018**, 90 (2018). https://doi.org/10.1186/s13661-018-1008-9
21. Baleanu, D., Mousalou, A., Rezapour, S.: On the existence of solutions for some infinite coefficient-symmetric Caputo–Fabrizio fractional integro-differential equations. Bound. Value Probl. **2017**, 145 (2017). https://doi.org/10.1186/s13661-017-0867-9
22. Ahmad, B., Alsaedi, A., Zahrah Nazemi, S., Rezapour, S.: Some existence theorems for fractional integro-differential equations and inclusions with initial and non-separated boundary conditions. Bound. Value Probl. **2014**, 249 (2014). https://doi.org/10.1186/s13661-014-0249-5
23. Rezapour, S., Esmael Samei, M.: On the existence of solutions for a multi-singular pointwise defined fractional *q*-integro-differential equation. Bound. Value Probl. **2020**, 38 (2020). https://doi.org/10.1186/s13661-020-01342-3
24. Baleanu, D., Agarwal, R.P., Mohammadi, H., et al.: Some existence results for a nonlinear fractional differential equation on partially ordered Banach spaces. Bound. Value Probl. **2013**, 112 (2013). https://doi.org/10.1186/1687-2770-2013-112
25. Samei, M.E., Rezapour, S.: On a system of fractional q-differential inclusions via sum of two multi-term functions on a time scale. Bound. Value Probl. **2020**, 135 (2020). https://doi.org/10.1186/s13661-020-01433-1
26. Hedayati, V., Samei, M.E.: Positive solutions of fractional differential equation with two pieces in chain interval and simultaneous Dirichlet boundary conditions. Bound. Value Probl. **2019**, 141 (2019). https://doi.org/10.1186/s13661-019-1251
27. Baleanu, D., Rezapour, S., Mohammadi, H.: Some existence results on nonlinear fractional differential equations. Philos. Trans. R. Soc. A, Math. Phys. Eng. Sci. **371**(1990), 20120144 (2013). https://doi.org/10.1098/rsta.2012.0144
28. Jajarmi, A., Baleanu, D.: A new iterative method for the numerical solution of high-order nonlinear fractional boundary value problems. Front. Phys. **8**, 220 (2020). https://doi.org/10.3389/fphy.2020.00220
29. Sajjadi, S., Baleanu, D., Jajarmi, A., Mohammadi Pirouz, H.: A new adaptive synchronization and hyperchaos control of a biological snap oscillator. Chaos Solitons Fractals **138**, 109919 (2020). https://doi.org/10.1016/j.chaos.2020.109919
30. Baleanu, D., Jajarmi, A., Sajjadi, S., Asad, J.H.: The fractional features of a harmonic oscillator with position-dependent mass. Commun. Theor. Phys. **72**, 055002 (2020)
31. Jajarmi, A., Yusuf, A., Baleanu, D., Inc, M.: New fractional HRSV model and its optimal control: a non-singular operator approach. Phys. A, Stat. Mech. Appl. **547**, 123860 (2020). https://doi.org/10.1016/j.physa.2019.123860
32. Baleanu, D., Jajarmi, A., Mohammadi, H., Rezapour, S.: A new study on the mathematical modelling of human liver with Caputo–Fabrizio fractional derivative. Chaos Solitons Fractals **134**, 109705 (2020). https://doi.org/10.1016/j.chaos.2020.109705
33. Jajarmi, A., Baleanu, D.: On the fractional optimal control problems with a general derivative operator. Asian J. Control (2019). https://doi.org/10.1002/asjc.2282
34. Veeresha, P., Prakasha, D., Baskonus, H., Yel, G.: An efficient analytical approach for fractional Lakshmanan–Porsezian–Daniel model. Math. Methods Appl. Sci. **43**, 4136–4155 (2020). https://doi.org/10.1002/mma.6179
35. Veeresha, P., Prakasha, D., Baskonus, H., Gao, W., Yel, G.: Regarding new numerical solution of fractional Schistosomiasis disease arising in biological phenomena. Chaos Solitons Fractals **133**, 109661 (2020). https://doi.org/10.1016/j.chaos.2020.109661
36. Gao, W., Senel, M., Yel, G., Baskonus, H., Senel, B.: New complex wave patterns to the electrical transmission line model arising in network system. AIMS Math. **5**(3), 1881–1892 (2020). https://doi.org/10.3934/math.2020125
37. Gao, W., Baskonus, H., Shi, L.: New investigation of bats–hosts–reservoir–people coronavirus model and apply to 2019-nCoV system. Adv. Differ. Equ. **2020**, 391 (2020). https://doi.org/10.1186/s13662-020-02831-6

38. Hairer, E., Lubich, C., Schlichte, M.: Fast numerical solution of weakly singular Volterra integral equations. J. Comput. Appl. Math. **23**(1), 87–98 (1988). https://doi.org/10.1016/0377-0427(88)90332-9
39. Friedlander, F.: The reflexion of sound pulses by convex parabolic reflectors. Math. Proc. Camb. Philos. Soc. **37**, 134–149 (1941). https://doi.org/10.1017/S0305004100021630
40. Rismani, A., Monfared, H.: Numerical solution of singular IVPs of Lane–Emden type using a modified Legendre-spectral method. Appl. Math. Model. **36**(10), 4830–4836 (2012). https://doi.org/10.1016/j.apm.2011.12.018
41. Gripenberg, G., Londen, S., Staffans, O.: Volterra Integral and Functional Equations. Cambridge University Press, Cambridge (1990)
42. Burton, T.: Volterra Integral and Differential Equations. Elsevier, Amsterdam (2005)
43. Brunner, H.: Collocation Method for Volterra Integral and Related Functional Equations. Cambridge University Press, Cambridge (2004)
44. Delves, L., Mohamed, J.L.: Computational Methods for Integral Equations. Cambridge University Press, Cambridge (1985)
45. Sezer, M.: Taylor polynomial solution of Volterra integral equations. Int. J. Math. Educ. Sci. Technol. **25**(5), 881–887 (1994). https://doi.org/10.1080/0020716051233133111 0
46. Ghasemi, M., Tavassoli, M., Bobolian, E.: Numerical solutions of the nonlinear Volterra–Fredholm integral equations by using homotopy perturbation method. Appl. Math. Comput. **188**, 446–449 (2007). https://doi.org/10.1016/j.amc.2006.10.015
47. Biazar, J.: GhazviniHe's homotopy perturbation method for solving system of Volterra integral equations of the second kind. Chaos Solitons Fractals **39**(2), 770–777 (2009). https://doi.org/10.1016/j.chaos.2007.01.108
48. Tahmasbi, A., Fard, O.: Numerical solution of linear Volterra integral equations system of the second kind. Appl. Math. Comput. **201**, 547–552 (2008). https://doi.org/10.1016/j.amc.2007.12.041
49. Han, B.: Framelets and Wavelets: Algorithms, Analysis, and Applications, Applied and Numerical Harmonic Analysis. Springer, Cham (2017)
50. Han, B., Michelle, M.: Construction of wavelets and framelets on a bounded interval. Anal. Appl. **16**, 807–849 (2018). https://doi.org/10.1142/S0219530518500045
51. Han, B., Lu, R.: Compactly supported quasi-tight multiframelets with high balancing orders and compact framelet transforms. arXiv preprint. arXiv:2001.06032 (2020)
52. Mohammad, M., Lin, E.B.: Gibbs phenomenon in tight framelet expansions. Commun. Nonlinear Sci. Numer. Simul. **55**, 84–92 (2018). https://doi.org/10.1016/j.cnsns.2017.06.029
53. Mohammad, M., Lin, E.B.: Gibbs effects using Daubechies and Coiflet tight framelet systems. Contemp. Math. **706**, 271–282 (2018). https://doi.org/10.1090/conm/706
54. Mohammad, M.: Special B-spline tight framelet and it's applications. J. Adv. Math. Comput. Sci. **29**, 1–18 (2018). https://doi.org/10.9734/JAMCS/2018/43716
55. Mohammad, M.: On the Gibbs effect based on the quasi-affine dual tight framelets system generated using the mixed oblique extension principle. Mathematics **7**, 952 (2019). https://doi.org/10.3390/math7100952
56. Mohammad, M.: Biorthogonal-wavelet-based method for numerical solution of Volterra integral equations. Entropy **21**, 1098 (2019). https://doi.org/10.3390/e21111098
57. Mohammad, M.: A numerical solution of Fredholm integral equations of the second kind based on tight framelets generated by the oblique extension principle. Symmetry **11**, 854 (2019). https://doi.org/10.3390/sym11070854
58. Mohammad, M.: Bi-orthogonal wavelets for investigating Gibbs effects via oblique extension principle. J. Phys. Conf. Ser. **2020**, 1489 (2020). https://doi.org/10.1088/1742-6596/1489/1/012009
59. Mohammad, M., Trounev, A.: Implicit Riesz wavelets based-method for solving singular fractional integro-differential equations with applications to hematopoietic stem cell modeling. Chaos Solitons Fractals **138**, 109991 (2020). https://doi.org/10.1016/j.chaos.2020.109991
60. Abdeljawad, T., Baleanu, D.: Integration by parts and its applications of a new non-local fractional derivative with Mittag-Leffler nonsingular kernel. J. Nonlinear Sci. Appl. **10**, 1098–1107 (2017). https://doi.org/10.22436/jnsa.010.03.20
61. Abdeljawad, T., Baleanu, D.: On fractional derivatives with exponential kernel and their discrete versions. Rep. Math. Phys. **80**(1), 11–27 (2017)